AD

AD-E403 531

Technical Report ARMET-TR-13042

MEASURING THE VELOCITY AND ORIENTATION OF MORTAR SHAPED PROJECTILES BY USING THE AUTOMATED COMPUTER VISION ANALYSIS METHOD

R. Decker
R. Hooke

June 2014

U.S. ARMY ARMAMENT RESEARCH, DEVELOPMENT AND ENGINEERING CENTER

Munitions Engineering Technology Center

Picatinny Arsenal, New Jersey

The views, opinions, and/or findings contained in this report are those of the author(s) and should not be construed as an official Department of the Army position, policy, or decision, unless so designated by other documentation.

The citation in this report of the names of commercial firms or commercially available products or services does not constitute official endorsement by or approval of the U.S. Government.

Destroy this report when no longer needed by any method that will prevent disclosure of its contents or reconstruction of the document. Do not return to the originator.

REPORT DOCUMENTATION PAGE

1. REPORT DATE (DD-MM-YYYY) June 2014	2. REPORT TYPE Final	3. DATES COVERED (*From - To*) February 2013 to May 2013

4. TITLE AND SUBTITLE	5a. CONTRACT NUMBER
MEASURING THE VELOCITY AND ORIENTATION OF MORTAR SHAPED PROJECTILES BY USING THE AUTOMATED COMPUTER VISION ANALYSIS METHOD	5b. GRANT NUMBER
	5c. PROGRAM ELEMENT NUMBER
6. AUTHORS	5d. PROJECT NUMBER
R. Decker and R. Hooke	5e. TASK NUMBER
	5f. WORK UNIT NUMBER

7. PERFORMING ORGANIZATION NAME(S) AND ADDRESS(ES) U.S. Army ARDEC, METC Fuze & Precision Armaments Technology Directorate (RDAR-MEF-E) Picatinny Arsenal, NJ 07806-5000	8. PERFORMING ORGANIZATION REPORT NUMBER

9. SPONSORING/MONITORING AGENCY NAME(S) AND ADDRESS(ES) U.S. Army ARDEC, ESIC Knowledge & Process Management (RDAR-EIK) Picatinny Arsenal, NJ 07806-5000	10. SPONSOR/MONITOR'S ACRONYM(S)
	11. SPONSOR/MONITOR'S REPORT NUMBER(S) Technical Report ARMET-TR-13042

12. DISTRIBUTION/AVAILABILITY STATEMENT

Approved for public release; distribution is unlimited.

13. SUPPLEMENTARY NOTES

14. ABSTRACT

   This is an attempt to extend the automated video analysis of artillery projectile launches to analyze mortar launches as well. Through simulations and synthetic video, the method is shown to be capable of quantifying mortar launches. Test video from a real test is also evaluated.

15. SUBJECT TERMS

Computer vision   Image processing   Artillery   Mortars   Launch video   Automated analysis
Pitch and yaw

16. SECURITY CLASSIFICATION OF:			17. LIMITATION OF ABSTRACT	18. NUMBER OF PAGES	19a. NAME OF RESPONSIBLE PERSON Ryan Decker
a. REPORT U	b. ABSTRACT U	c. THIS PAGE U	SAR	21	19b. TELEPHONE NUMBER (Include area code) (973) 724-7789

CONTENTS

FIGURES

FIGURES
(continued)

UNCLASSIFIED

ACKNOWLEDGMENTS

INTRODUCTION

Like artillery projectiles, mortar munitions have complex aerodynamics that need to be well characterized for soldiers to use them effectively. Routine testing is conducted during the development of mortars to measure aerodynamic performance and accuracy. Following launch from a gun tube, the mortar projectile relies on the fins on its base to pull its center of pressure behind its center of gravity in order to ensure static and dynamic stability. During this phase where the mortar goes from being confined in the tube to relying on its fins for stable flight, the body of the mortar may exhibit large yaw behavior. The quicker the projectile stabilizes (and the less initial pitch and yaw the projectile exhibits) contribute to increasing the accuracy and range of the weapon.

This report is an effort to quantify the initial velocity and orientation behavior of an artillery mortar from launch video. In previous work, a method was developed to automatically measure the initial pitch and yaw history of an artillery projectile (ref. 1). Subsequent testing showed the method was able to match conventional data reduction methods to within a degree (refs. 2 and 3). For mortars, however, the geometry is not quite as simple as the bullet-shape of a projectile. Therefore, a new shape model was developed as well as a new algorithm for robustly measuring the pitch or yaw angle of the projectile in each image frame. Results from an initial test are included to evaluate the performance and potential of the automated method for measuring both the velocity and the total (spatial) angle of attack of a mortar in free flight.

SEGMENTATION PROCEDURE AND OBSERVED PITCH ANGLE CALCULATION FOR MORTAR SHAPES

The automated launch video analysis method works by loading in high-speed video of projectile launches. The analysis is capable of extracting important data from a video file such as the time, frame-rate, and number of frames from any image in the video (if made using a Photron SA FastCam) by employing optical character recognition techniques. The algorithm then steps through each frame of the launch video and uses edge detection and morphological operations to identify candidate shapes. The sequential process of segmenting the largest shape is shown in figure 1.
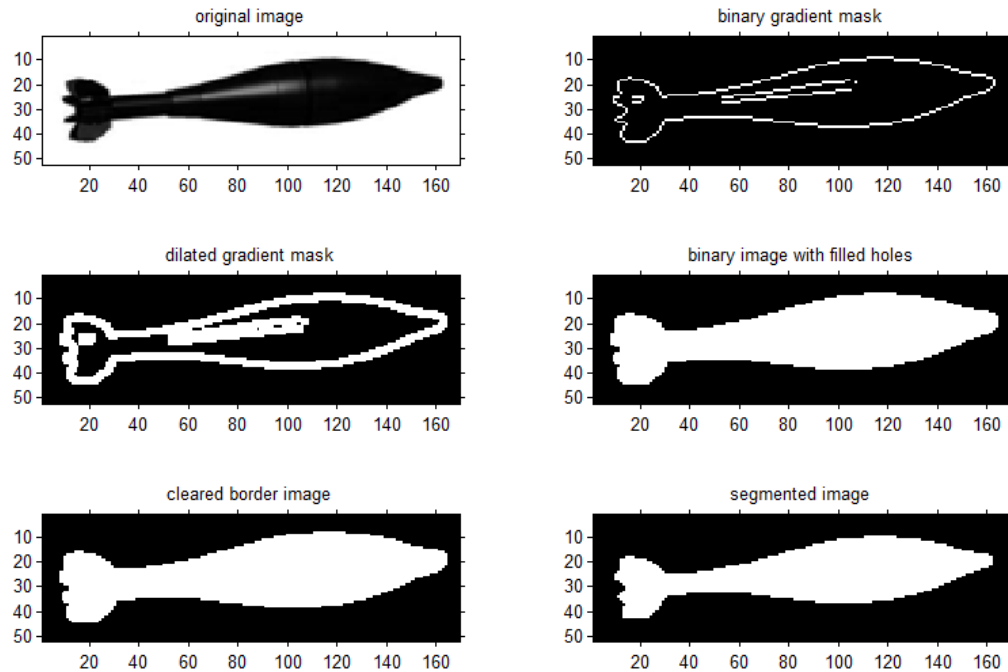
Figure 1
120 mm-type mortar shape segmentation process

The largest shape identified in the image is then geometrically analyzed to measure its orientation in the image frame. This process begins by finding the central moment location of all pixels that constitute the candidate shape. The row and column pixel locations are then subtracted from the central moment location and converted to polar coordinates for shape analysis. This is a critical step in developing a precise and robust measurement of the shape's pitch angle in an image. Figure 2a illustrates the simpler polar distribution of the pixels in an artillery projectile shape, as compared to the polar distribution of pixels of a mortar projectile shape (fig. 2b).

(a) Projectile shape   (b) Mortar shape
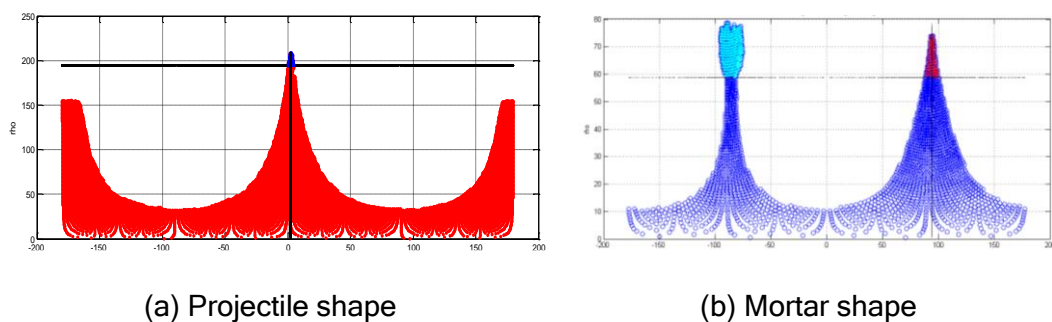
Figure 2
Polar pixel distribution projectile and mortar shapes

In the case of the artillery projectile (fig. 2a), it is easy to threshold the distance of pixels from the central moment to identify the nose region. For the mortar, thresholding the 20% of pixels that are farthest from the centroid results in the identification of both the nose and the tail fin regions. Since the tail is always represented by a larger area than the nose/ogive region, the two groups can be classified according to the number of pixels. However, since the videos are preconditioned so that the projectile points to the right, it is easier to classify the two groups by their relative location to the

left or right of the projectile central moment. If it was desired to analyze unstable rounds as they tumble, then a different approach would need to be used.

After the nose and tail pixel groups are classified, a precise pitch angle can be calculated as the average of polar angles that each pixel in either group makes relative to the central moment. Since glint from the sun frequently interferes with the segmentation process near the fuze (located at the nose), it has been found that using the tail group of pixels is more robust, especially for low resolution video. Minor deflections of metal parts on the mortar projectiles are assumed to be negligible due to low aerodynamic forces and a thorough understanding of the design.

MORTAR SHAPE MODEL

The candidate shape is now ready to be analyzed to determine if the object found is a mortar. To do this, the computer must first be taught what a mortar looks like using an active shape model (ASM) (ref. 4) specific to a certain mortar shape. The pixels along the border of the shape are rotated by the observed orientation angle found in the previous step so that the shape points directly to the right. The edge pixel locations are then centered about the central moment and normalized by the length of the shape as shown in figure 3.
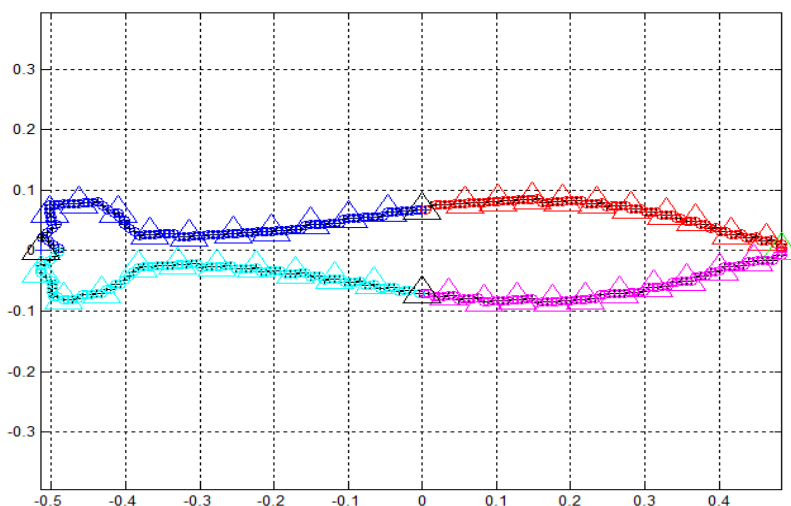
Figure 3
Normalized edge pixels for ASM comparison

The edge pixels are separated into four quadrants. They are numbered sequentially in each quadrant using a nearest neighbor algorithm in the counter-clockwise direction. Launch videos from test to test often vary significantly in size and resolution depending on the test site, gun position, and video and processing equipment used. Therefore, of the hundreds of edge pixels, only ten are taken from each quadrant to constitute the ASM. In figure 3, the pixels used for the ASM (also known as tags) are identified by large triangles.

To build the ASM, this process is repeated for every image in the training set (fig. 4). These images are generated from 3D computer models of mortars and represent different view angles or presented areas of the projectile relative to the camera that may be observed in real launch videos. From the tags generated for each of these 120 mm-type mortar shapes, an average shape is then calculated. The principal modes of shape variation of the mortar images are determined using principal component analysis. The mean image and three largest modes of variation found for the training set in figure 4 are illustrated in figure 5.
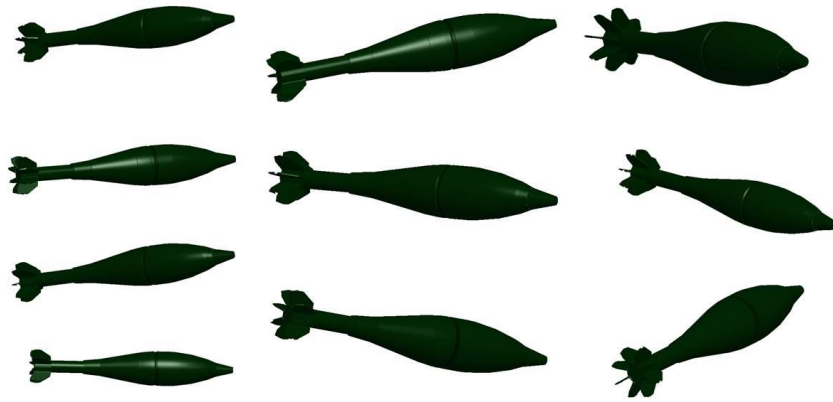
Figure 4
Mortar shape training set
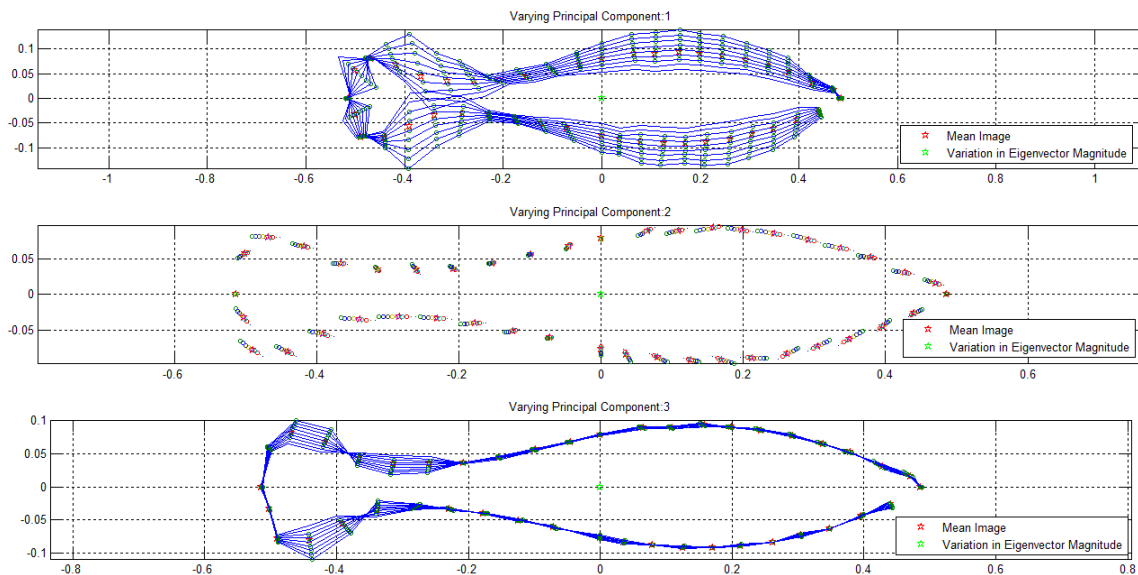
Figure 5
Modes of variation for 120 mm-type mortar training set

Statistical analysis of the ASM has shown that over 90% of the shape digression can be characterized by varying only the first mode of variation. As illustrated in figure 5, the length-normalized shape appears to get fatter or skinnier in the first variation mode depending on the perpendicularity of the view angle. The second mode appears to be the result of slight shifts in tag locations caused by the sampling process, and the third mode appears to account for different appearances of the tail fins due to projectile rotation. For simplicity, only the mean image and the first component are used to classify the candidate shape as representing a 120 mm-type mortar. If the coefficient that corresponds to the first mode of variation has a value lower than three, then the shape is classified and the segmentation procedure is complete. If not, the edge detection sensitivity is increased and the process runs as many as 20 times for each video frame before the analysis terminates and exits, reporting that no mortar shape was found in that image frame.

FIELD TESTING

In May 2013, a field test took place at the Naval Surface Warfare Center (NSWC) at Dahlgren, VA. The purpose of the test was to evaluate a sequence of different obturator designs in terms of their ability to decrease the variability in range of a 120-mm mortar system at low charges. In addition to measuring the range of the mortars fired, the test team sought to collect muzzle velocity measurements, tube pressures, and quantify the initial yaw. This was to help them in selecting the most effective obturator designs, which minimize the exaggeration of initial pitch and yaw rates that have been previously identified in the system.

CAMERA SETUP AND CALIBRATION

The facility at NSWC was not equipped with two Trajectory Tracker (TT) (ref. 5) moving-view optical systems that have been used previously with the automated pitch and yaw measurement of artillery projectiles at Yuma Proving Grounds, AZ. Instead, two high-speed Phantom (models 640 and 341) fixed-view cameras were used to record the initial portion of flight as shown in figure 6a, where the mortar tube is visible in the background. Each camera was located approximately 14.5 m downrange and 14.5 m off of the azimuth of fire, as shown in figure 6b, to give an orthogonal view of the mortars along their line of fire after muzzle exit.

(a)
Camera setup
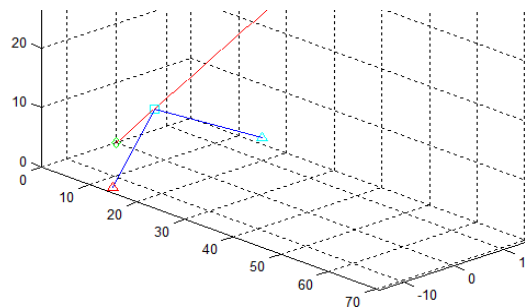
(b)
Launch geometry

Figure 6
Camera setup showing camera and launch geometry

The central axis of the camera was oriented to observe a point 19 m from the tube muzzle, which was the location where aeroballistic analysis predicted the maximum pitch and yaw to occur (average of maximum yaw locations for several different launch velocities). Although the field of view was narrow, approximately 15 m of flight along the line of fire was able to be recorded by each camera. The cameras were set to record at 3,000 frames per second, which allowed 150 to 450 images of the mortar to be captured during each shot, depending on the projectile velocity.

The camera calibration algorithm described in reference 3 was used to correct the lens aberrations of the fixed-view cameras. A sequence of 11 images was captured using a wide calibration pattern as shown in figure 7a. To capture more mortar images, a longer segment of flight was needed, and an extra-wide resolution of 2560 by 452 was used to achieve this field of view. Even for the wider calibration target, this extra-wide resolution required that the calibration set include images of the calibration target at the far leftmost and far rightmost regions of the field of view. A projection of the calibration target orientations is also shown in figure 7b. To determine the number of radians per pixel in the image, a 5-m calibration beam was used (fig. 7c).
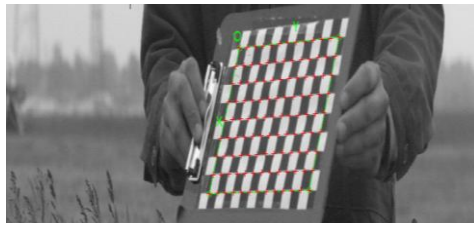
(a)
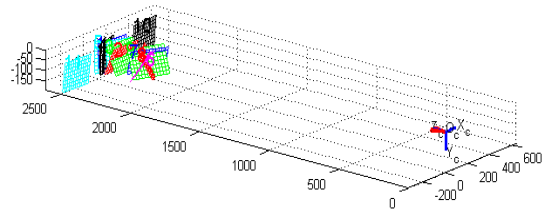
(b)

(c)

Figure 7
Camera calibration image sample (a), extrinsic projection of calibration images (b), and determining the number of radians per pixel (c)

ASSESSMENT OF LOW RESOLUTION VIDEO

Due to the distance between the cameras and the line of fire, a lower-than-usual resolution was expected. A sensitivity analysis had previously been conducted on the ability of the automated video analysis method to function correctly at lower resolutions. From this analysis, which used perfectly conditioned synthetic video (not real video), the lowest resolution found to accurately segment and measure the orientation of projectile within a degree was 125 pixels along the projectile axis. For mortar field test, the available telephoto lenses limited the resolution to between 110 and 120 pixels along the axis of the projectile as illustrated by the sample video frame and pixel resolution history images in figure 8.
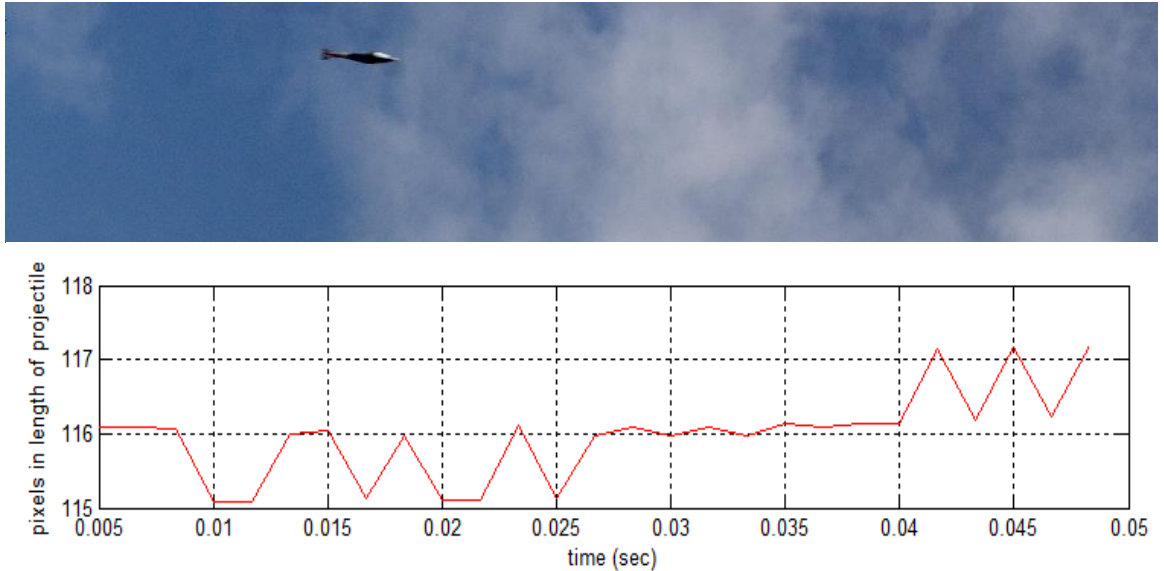
Figure 8
Sample video frame and mortar resolution

Comparatively, TT and Flight-Follower (ref. 6) videos previously used in the analysis of artillery projectile launches typically yield resolutions between 200 and 450 pixels along the axis of the projectile. In addition, real videos are subject to glint and imperfect focus that further degrade the analysis, making the low resolution even more problematic for accurately measuring pitch and yaw. Figure 9 shows a properly segmented mortar shape from one of the videos.
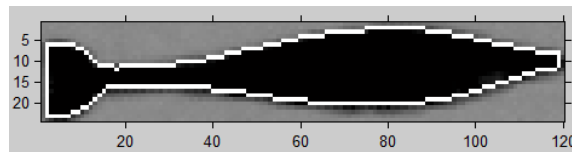
Figure 9
Properly segmented mortar shape

Unfortunately, approximately half of the frames analyzed for the launches in this test resulted in an unsatisfactory segmentation. The authors accredit this problem mostly to the low resolution available during the test event. Lighting conditions also contributed to this problem, as the glint from the sun caused the top of the projectile to blend in with the image background. When the segmentation algorithm neglects pixels on the top of the mortar shape due to boundary diffusion, the observed pitch angle estimate is lower than the real projectile orientation in the image frame. Since this issue was more common for videos recorded from the left camera (looking downrange from the weapon), this had the overall effect of biasing the readings significantly toward the negative pitch (down) and positive yaw directions (left). Figure 10 contains images of poorly segmented video frames. It is difficult to quantify exactly how much bias this effect introduces in the overall analysis and the derived pitch and yaw angles.
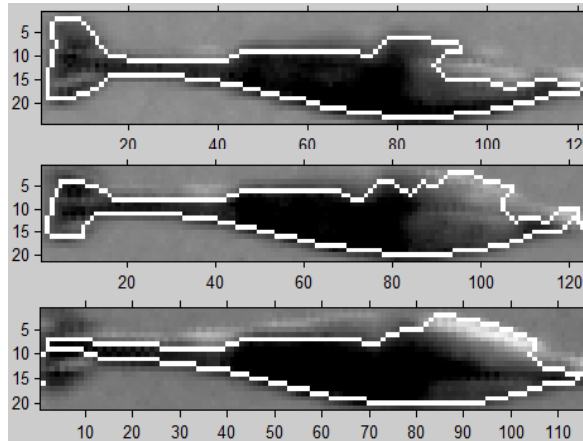
Figure 10
Poorly segmented mortar shapes

ASSESSMENT OF CALIBRATION

The mathematical significance of the camera calibration step is that the distortion correction should result in an image where a certain number of pixels in a row or column equate directly to a corresponding number of radians in the field of view. This allows an accurate conversion from pixels within the frame to radians relative to the polar coordinate system of the frame. Since this test used fixed-position cameras and the mortars follow a ballistic path, the motion of the projectile should follow a straight line in the undistorted field of view. Therefore, the time-history of the central moment location in each frame of the video should show a linear change in the column number as the projectile passes though the field of view (fig. 11). In this short amount of time, the projectile velocity deceleration is insignificant and gravity effects can be ignored.
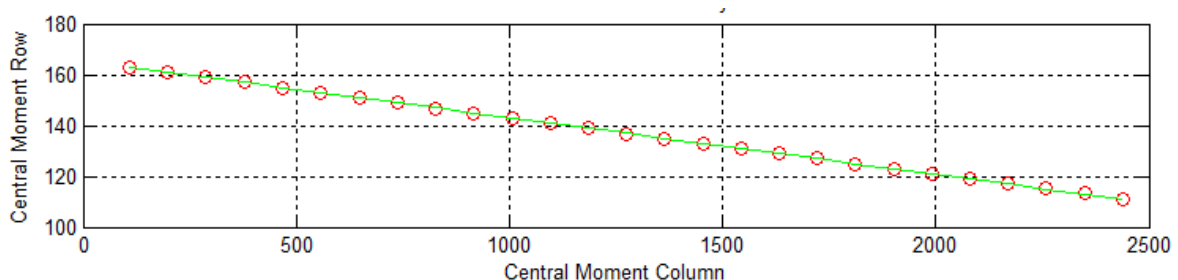
Figure 11
Projectile location in each video frame

For one of the sample videos that exhibited results of acceptable segmentation quality (tube round no. 3), the linear motion through the columns was investigated. The videos from both cameras were analyzed with and without the camera distortion correction algorithm. The results of this assessment are shown in table 1. The analysis required 3 min and 22 sec while running on a laptop computer in MATLAB (ref. 7) after downgrading the analysis from 3,000 to 1,500 frames per second (fps).

Table 1
Results of lens correction investigation

Video Version	Measured Velocity (m/s)	Radar Data Velocity (m/s)	% Error	Linear Fit R^2 Value
Left Camera Distorted	84.53	86.1	-1.83%	0.9786
Right Camera Distorted	87.53	86.1	1.67%	0.9989
Left Camera Corrected	84.40	86.1	-1.97%	0.9361
Right Camera Corrected	87.82	86.1	2.00%	0.9945

In a previous attempt to improve results using the camera calibration algorithm, no evidence was found that the calibration effort was beneficial (ref. 8). From the data in table 1, there is once again no indication that the lens correction is producing a better analysis result. From the comparison of the velocity estimates computed using the automated computer vision analyis method to the actual radar velocity measurement, for each camera, the computed velocities with lens correction yielded larger errors than the estimates from the uncorrected videos. When a linear equation was fit to the central moment history from each of the four videos, the original distorted videos yielded a better coefficient of determination (R^2) fit to a straight line than the distortion corrected videos. The right camera, in particular, exhibited a good fit to a linear projectile movement. This could be explained by the fact that the left camera incurred more glint and exhibited poorer focus leading to partial shape segmentation.

VELOCITY ANALYSIS RESULTS

Knowledge of the measured distance to the 5-m calibration beam in figure 7c resulted in the relationship that each pixel was equivalent to 0.000203 rad in the field of view. Using this relationship, the average angular velocity of the projectile in each video was determined by examination of how far the mortar projectile's central moment changed between adjacent video frames. These estimates between adjacent frames were then sorted and the median 50% of estimates were averaged to find the average angular velocity and to discard erroneous results and outliers. Muliplying this value by the distance from the camera to the line of fire resulted in a velocity estimate for each camera. For each round analyzed, the velocity estimates from the left and right cameras were averaged to output a single result. Future code estimates may allow one to bias one camera or another to account for issues experienced during testing once the results have been validated.

For the most part, the results were close to the estimates measured by radar. In fact, for the first 20 shots, 16 rounds resulted in velocity estimates that were within 0.5 m/s (approximately 0.3% error). However, the velocity results exhibited gross errors for 15 of the 80 total shots and yielded no velocity estimates for three shots in this test. As the test progressed, it appeared that the velocity estimates (excluding the gross errors) began to incrementally drift farther from the radar velocity estimates (fig. 12). This could be the result of movements in the camera, changes in the mortar tube orientation, retreat of the origin of flight and ballistic path as the weapon burried itself during testing, or slight changes in the camera zoom even though the focus was taped in place as shown previously in figure 6a. Since a variety of muzzle velocities were used during this test, the error assessment is shown to display both total magnitude of the difference between the automated analysis estimate and the radar measurement, as well as the percentage error difference.
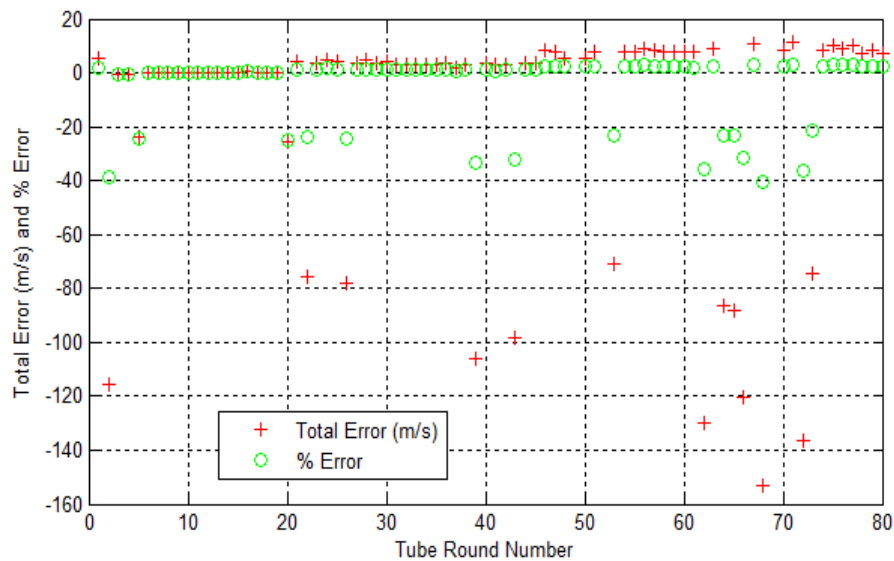
Figure 12
Error in velocity estimate

The results that exhibited gross errors may have been caused by incorrect handling of dropout frames or problems reading the inter-range instrumentation group time signals using a custom optical character recognition method (ref. 9) in some of the videos. It is uncertain if this was occurring more often in either the left or right cameras. This problem will be explored further in future efforts. In all cases of gross errors, the estimates were below the radar velocity estimate.

PITCH AND YAW RESULTS

For the 62 shots that delivered reasonable velocity estimates, the automated analysis also delivered reasonable estimates for pitch and yaw, resulting in total (spatial) angle of attack estimates that ranged from 0.72 to 12.03 deg. Spin-stabilized projectiles exhibit epicyclic motion behavior at high frequencies. Fin-stabilized mortars also exhibit similar behavior but at rates too slow to capture in the duration of the fixed-view launch video. Therefore, the results for most of the shots look like the alpha-beta (pitch/yaw) plot in figure 13a. It should be noted that for fin-stabilized projectiles, the nutation and precession oscilliations occur in opposite directions whereas, for spin-stabilized projectiles, both oscillations occur in the same direction of the spin-rate (ref. 10).

(a)   (b)
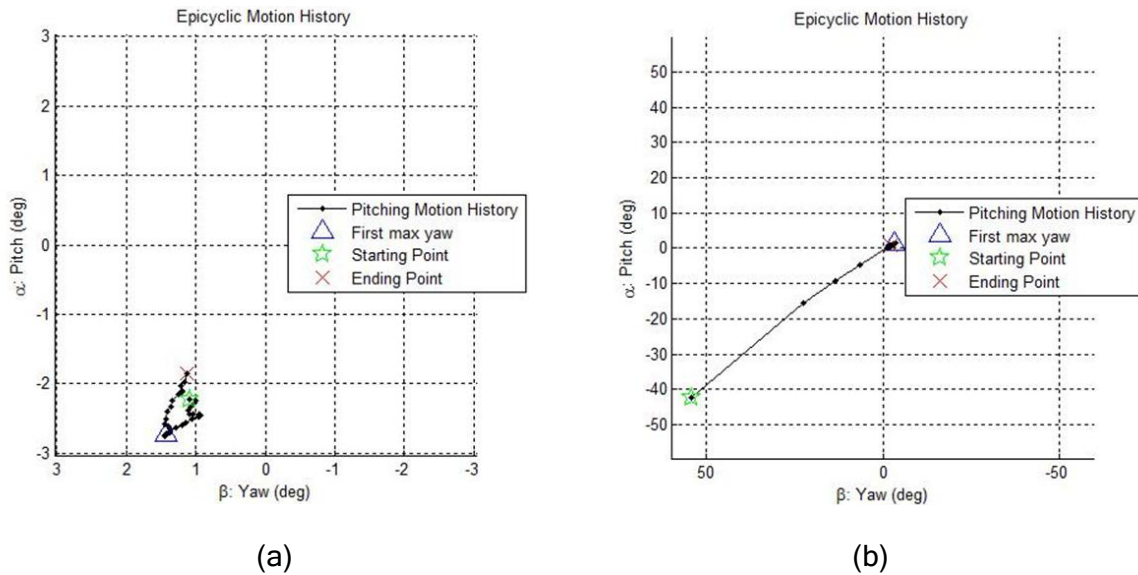
Figure 13
Alpha-beta plots for a correctly automated result (a) and a result with extraneous initial data points
due to partial segmentation (b)

For nearly half of the rounds where the velocity estimate was poor, falsely high angle of attack results were found. Using the alpha-beta plots, reasonable corretions were manually conducted to deliver a final result. The alpha-beta plot in figure 13b illustrates one of the results where the initial pitch and yaw estimates were incorrect (likely due to partial segmentation). The final angle of attack results for 76 of the 80 rounds fired (fig. 14). There were four videos where manually revisiting the plots did not yield an answer.

Figure 14
Angle of attack results for entire test

CONCLUSIONS

The most important result from this test was that it was shown that the mortar shape can be found using the automated video analysis method. In addition, it was shown that the method can be used on fixed-view cameras, meaning that with proper image resolution, manual data reduction could eventually be replaced. In the future, a direct comparison between manually reduced fixed-view video and results from the au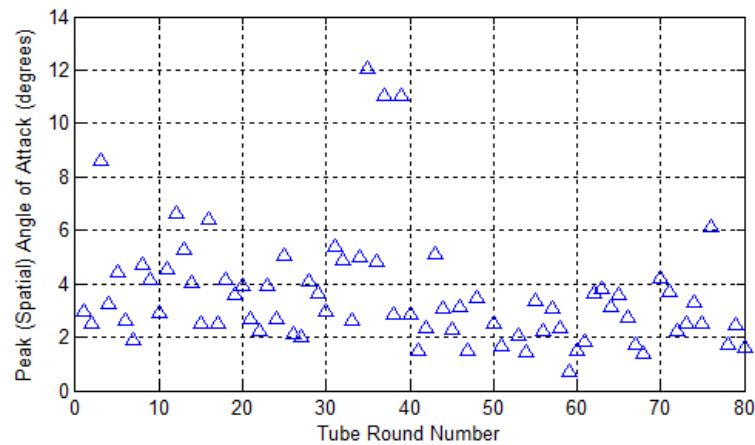tomated video analysis method should be conducted. Hopefully, with sufficient resolution and an improved camera lens correction, velocity measurements from launch video will become more accurate as well.

A significant lesson learned during this effort was that resolution and image clarity play a considerable part in the accuracy of the segmentation algorithm. A more advanced segmentation algorithm based on the active shape model could be implemented. It may slow down the analysis but could have significant effects on the accuracy of the results. Further research into lens filters and camera settings may yield images that do not have segmentation drop out.

DISCUSSION AND RECOMMENDATIONS FOR FUTURE TESTING

The results of the velocity analysis show that with improvements, a velocity measurement using a fixed-view launch video is possible, even with a low number of pixels along the projectile axis. The feasibility of measuring projectile pose for mortars was also demonstrated but, unfortunately, there were no alternative approaches employed on this test for verification of results.

Spin-rate methods in development (ref. 11) may also be applied to this problem. For such slow spinning rounds, however, it will be necessary to paint more than six stripes on a mortar to use the slow-spinning automated algorithm that works best when more than eight stripe boundaries are detected (ref. 12). In the videos during this mortar test, only one to four boundaries were observed.

Improving the resolution on the next test should be the first priority. If testing at a test site that is equipped with multiple Flight-Follower or Trajectory Tracker systems, then those systems should be considered. If only fixed-view cameras are available, it would be advantageous to move the cameras closer to the azimuth of fire to improve projectile resolution. The tradeoff would be a reduced number of data points but, at a high frame-rate of 3,000 fps, there will still be more than enough data points to quantify both orientation and velocity.

Improvements to the calibration process should also be made. These may include using more calibration images of an even wider target and calibrating with a larger target located farther from the camera.

Once satisfactory results have been proven, it is plausible to extend this automated video analysis method beyond artillery and mortars to missiles, rockets, and complicated projectiles such as sabot rounds.

REFERENCES

1. Decker, R., Kölsch, M., and Yakimenko, O. A., An Automated Method for Computer Vision Analysis of Cannon-Launched Artillery Video, *Proceedings of the 27th International Ballistics Symposium*, presented at the 27th International Ballistics Symposium, Freiburg, Germany, (2013c).

2. Decker, R., Yakimenko, O. A., and Kölsch, M., *Artillery Pitch and Yaw Measurement Test Report: An Automated Video Analysis Method to Measure First Maximum Yaw* , Technical Report no. ARMET-TR-13026, U.S. Army ARDEC, Picatinny Arsenal, NJ, May 2014.

3. Decker, R., Harkins, T., and Davis, B., *Pitch and Yaw Trajectory Measurement Comparison from Automated Video Analysis and On-Board Sensor Data Analysis Technique*, Technical Report no. ARL-TR-6576, U.S. Army Research Laboratory, Aberdeen Proving Ground, MD, September 2013.

4. Cootes, T. F., Taylor, C. J., Cooper, D. H., and Graham, J., Active Shape Models – Their Training and Application, *Computer Vision and Understanding*, *61*(1), 38-59, 1995.

5. Decker, R., "A Computer Vision-Based Method for Artillery Characterization," Naval Postgraduate School, Monterey, CA, Doctoral Dissertation, December 2013.

6. Specialised Imaging, *Trajectory Tracker User Manual* (User Manual), Temecula, CA, 2012.

7. Itronix, *DRS's Flight Follower System* (Specification Sheet), retrieved from www.itronix.com/pdf/DRS_Flight_Follower.pdf, 2012.

8. *MATLAB*, Natick, Massachusetts: The MathWorks Inc., 2011.

9. Saroch, A., *Optical Character Recognition*, The MathWorks Inc., 2010.

10. Carlucci, D. and Jacobson, S., *Ballistics: Theory and Design of Guns and Ammunition*, Boca Raton, FL: CRC Press, 2008.

11. Decker, R., Kölsch, M., and Yakimenko, O. A., *A Computer Vision Approach to Automatically Measure the Spin-rate of Artillery Projectiles Painted with Stripes*, Monterey CA: Naval Postgraduate School, 2012.

12. Decker, R., Kölsch, M., and Yakimenko, O. A., *A Computer Vision Approach to Automatically Measure the Spin-rate of Fin-Stabilized Projectiles Painted with Stripes*, Monterey CA: Naval Postgraduate School, (2013b).

DISTRIBUTION LIST

U.S. Army ARDEC
ATTN: RDAR-EIK
         RDAR-GC
         RDAR-MEF-E,   R. Decker
                         R. Hooke
Picatinny Arsenal, NJ 07806-5000

Defense Technical Information Center (DTIC)
ATTN: Accessions Division
8725 John J. Kingman Road, Ste 0944
Fort Belvoir, VA 22060-6218

GIDEP Operations Center
P.O. Box 8000
Corona, CA 91718-8000
gidep@gidep.org

REVIEW AND APPROVAL OF ARDEC TECHNICAL REPORTS

Using the Automated Computer Vision Analysis Method to Measure the Velocity and Orientation of
Mortar Shaped Projectiles
Title

_____
Date received by LCSD

Ryan Decker   ARMST-TR-13042
Author/Project Engineer   Report number (to be assigned by LCSD)

(x7789)   Building 94   RDAR-MEF-E
Extension   Building   Author's/Project Engineers Office
                                               (Division, Laboratory, Symbol)

PART 1. **Must be signed before the report can be edited.**

a.   The draft copy of this report has been reviewed for technical accuracy and is approved
      for editing.

b.   Use Distribution Statement A_X__, B__, C____, D____, E____, F____ or X____ for the reason
      checked on the continuation of this form.

      1.   If Statement A is selected, the report will be released to the National Technical
            Information Service (NTIS) for sale to the general public. Only unclassified reports
            whose distribution is not limited or controlled in any way are released to NTIS.

      2.   If Statement B, C, D, E, F, or X is selected, the report will be released to the Defense
            Technical Information Center (DTIC) which will limit distribution according to the
            conditions indicated in the statement.

c.   The distribution list for this report has been reviewed for accuracy and completeness.

                        Robert Lee   for Doug Troast 8/9/2013
                        Division Chief   (Date)
_____

PART 2. To be signed either when draft report is submitted or after review of reproduction copy.

        This report is approved for publication.

                        Douglas C. Troast   13 June 2014
                        Division Chief   (Date)

SMCAR Form 49, 20 Dec 06 supersedes SMCAR Form 49, 1 Nov 94.

                        Stephen Leong   29 JUN 2014
                        RDAR-CIS   Date